PAPER • **OPEN ACCESS**

Power-to-liquid versus biomass-derived kerosene: a comparative study

To cite this article: Giovanni Manente *et al* 2023 *J. Phys.: Conf. Ser.* **2648** 012018

Power-to-liquid versus biomass-derived kerosene: a comparative study

Giovanni Manente, Antonio Ficarella, Ahtasham Rahim

Department of Engineering for Innovation, University of Salento, Lecce, Italy

Corresponding author: giovanni.manente@unisalento.it

Abstract. Power-to-Liquid (PtL) kerosene is considered by many experts as the only viable option to achieve a large scale decarbonization of the aviation sector in the near-medium term. In the PtL process carbon dioxide of renewable origin or from ambient air and green hydrogen are combined to produce a liquid fuel that can replace fossil kerosene. For this purpose the Fischer-Tropsch pathway and the methanol pathway are available. On the other hand, more production pathways are available when using a biomass feedstock. The aim of this work is to compare the power and biogenic routes for the production of sustainable kerosene in terms of performance and requirements. Indeed, there is a lack of studies in the literature that directly compare the two options, i.e. biofuels and e-fuels, on a common basis. Accordingly, simulation models are built in this work for both routes to calculate the yield of kerosene and co-products, the hydrogen demand, the flows of carbon dioxide, the electricity and thermal energy demands. The simulation outputs are compared against the results of the relevant studies in the literature. The expectation from this comparative study is to highlight the criticalities of each route and, possibly, any opportunity to overcome them by exploring any synergy between the different routes.

1. Introduction

The production of sustainable aviation fuels (SAF) can be based on either the biological route or the synthetic route. Among the biological routes the gasification-Fischer Tropsch (G-FT) appears one of the most promising because it combines the conversion of waste biomass using a mature technology, like gasification, with the Fischer Tropsch (FT) synthesis, which is an emerging technology for the biomass field. On the other hand, the e-fuel production leverage the standard FT technology using a clean syngas produced from green hydrogen and CO_2 captured from air or concentrated sources. Thus, it appears that a common treatment of these two alternatives is possible by isolating the syngas generation section from the jet fuel production section. In the former, biomass gasification and the reverse water gas shift reaction represent the two alternative options for syngas production. In the latter section, the FT synthesis represents the single technology which is employed in both pathways. The aim of this work is to highlight this connection in the production of bio-kerosene and e-kerosene, which is often overlooked. The method consists in analyzing different techno-economic studies about both pathways and identifying any similarity in the modelling approaches. After a deep analysis of the literature, a modelling strategy is selected and applied to model both the main processes in the production of bio-kerosene and e-kerosene.

2. The Gasification-Fischer Tropsch route for the production of bio-kerosene

This section deals with the critical analysis of the most relevant techno-economic studies about the gasification-Fischer Tropsch route for the production of bio-kerosene. The focus is on the modelling approaches used for the simulation of the biomass gasification and Fischer-Tropsch synthesis, which appear the most critical.

2.1. Biomass feedstock

Different biomass resources have been considered for the gasification-FT processes, as summarized in Table 1. In many papers a generic lignocellulosic or woody biomass is considered (Tuna, 2014)(Spyrakis, 2009). A specific biomass resource (e.g. switchgrass, corn stover, etc.) is selected in other studies based on wide availability and/or low cost, taking average property data from the literature (see e.g. (Larson, 2009)(Swanson, 2010)). In only few studies, the biomass properties needed as input for the techno-economic analysis are experimentally determined for a specific feedstock (e.g. rice husk), through elemental and thermogravimetric analysers (Wang, 2022). Due to the inclusion of the FT process, which is considered viable and efficient only at large scales, and the significant reductions in unit capital cost that accompany increasing plant size, the throughputs considered for these G-FT systems is typically large, in the order of a few thousand tons per day. However, the recent interest in scaling-down the FT technology to better match the limited and unpredictable availability of biomass finds some evidence in studies, like in (Snehesh, 2017), where the plant capacity is reduced by two orders of magnitude.

Table 1. Biomass resources, feed rates and feed energy inputs of different studies on gasification-FT.

Biomass resource	Feed rate (dry basis)	Feed energy input (MW_{th})	Reference
Poplar wood chips	80 tons/hour	367 (LHV_{wet})	[1]
Willow wood	26.5 kg/s	421 (LHV)	[2]
Switchgrass	4536 tons/day	893 (LHV)	[3]
Corn stover	2000 tons/day	389 (LHV)	[4],[5]
Woody biomass	1 ton/hr	4.3 (LHV)	[6]
Pine chips	2000 tons/day	N.A.	[7]
Woody biomass	N.A.	400 (HHV)	[8]
Sugarcane residues (trash and bagasse)	66.4 tons/hour	331 (HHV)	[9]
Rice straw	80 tons/hour	393 (HHV)	[10]
Lignocellulosic biomass	77.9 tons/hour	N.A.	[11]
Casuarina wood-chips	1 ton/hour	4.9	[12]
Rice husk	600 tons/day	98.3	[13]

2.2. Biomass gasification

Conversion of biomass to an H_2 and CO containing feed gas that is suited for FT synthesis takes places through gasification. The biomass gasification technology that is mostly considered for syngas production in G-FT plants is the fluidized bed gasification. Within this technology different options based on direct/indirect gasification, air blown/oxygen blown and atmospheric/pressurized have been explored. Some studies refer to specific fluidized bed gasifiers developed and tested (often at pilot scale) for the same biomass resource by given manufacturers or research institutes. In these cases the syngas composition, yield and gasifier efficiency are known and applied straight as inputs in the techno-economic analysis [1] [8]. In other studies the empirical data of syngas composition for pilot plant operation of the gasifier are used as input to adjust the chemical equilibrium model-based predictions [3] [6]. Alternatively, the gasifier product distribution obtained by the experiments was adjusted in [5] to verify the elemental mass balance across the gasifier. A purely numerical approach is applied in other studies, where the syngas composition is calculated by using a chemical equilibrium based model like in [9] or a kinetic-based model like in [10]. This is done only after the verification of a good agreement between the model predictions and the experimental data in the literature obtained using the same biomass feedstock and under the same operational conditions.

For small scale G-FT systems the downdraft gasifier technology is typically considered, mainly due to the low amount of tar in the produced syngas. In [12] the average syngas composition and yield obtained in the lab-scale downdraft gasifier were used straight as inputs for the techno-economic analysis of a scaled up system, having a throughput 100 times higher yet based on the same gasification technology. In [13] the same syngas yield and composition are applied somehow arbitrarily to a much larger system (where the downdraft technology is not viable) and a different biomass feedstock. Furthermore, the use of a chemical reactor model (RYield) that requires a mass balance only but not an atom balance appear questionable, given that the properties of the biomass feedstock were known.

In [1] a theoretical case is examined where the steam to biomass ratio is increased and the pressure is decreased compared to a reference pressurized oxygen blown gasifier, in order to reach a more optimum H_2:CO ratio for

the FT reactor. In [9] the steam to biomass ratio and oxygen to biomass ratio are varied in a wide range in order to reach the target temperature and a H_2/CO equal to 2. The optimum gasification parameters were selected as those that maximized the conversion efficiency and minimized the cost of syngas production. In [12] the steam to biomass ratio was maintained in the range of 0.8-1.2, to achieve syngas with H_2/CO of 2.1:1, which is an ideal case for cobalt based FT system.

Table 2. Gasifier type, operating conditions and performance considered in gasification-FT studies.

Gasifier technology	Gasifier process type	Gasifier temperature (°C)	Mass ratio oxygen/air to biomass	Mass ratio steam to biomass	Gasifier efficiency (%)	H_2/CO molar ratio	Tar yield	Ref.
Circulating Fluidized Bed (CFB)	a) Direct air-blown atmospheric; b) Direct air-blown pressurized; c) Direct oxygen blown pressurized; d) Indirect air-blown atmospheric.	a) 900; b) 950; c) 968-982; d) 863.	a) 1.4 (air); b) N.A.; c) 0.3; d) 1.46 (air)	a) 0.34; b) 0.34; c) 0.34-0.6; d) 0.19	a) 80 b) 88.6 c) 80.8 d) 86.8 (LHV)	a) 0.77; b) 0.73; c) 1.39-2.0; d) 0.45	Not known, but order of magnitude is g/Nm^3	[1]
Circulating Fluidized Bed (CFB)	a) Direct airblown atmospheric/pressurized; b) Direct oxygen blown atmospheric/pressurized	a) 850; b) 850	a) 1.06-1.23 (air); b) 0.21-0.26	a) 0; b) 0.32-0.42	N.A.	N.A.	1.5 wt.% of the dry feed	[2]
Circulating Fluidized Bed (CFB)	Direct oxygen-blown pressurized	1003	0.267	0.210	79.8 (LHV)	1.72	1 wt.% of the dry biomass	[3]
Fluidized bed	Direct airblown atmospheric/pressurized	800	1.73 (air)	0	N.A.	N.A.	5 g per Nm^3 of syngas	[6]
Circulating Fluidized bed (CFB)	Direct oxygen-blown pressurized	870	0.26	0.17	68.8 (LHV)	0.83	500 ppm (mole fraction)	[4] [5]
Entrained flow	Pressurized, oxygen-blown	1300	0.35	0.48	87.9 (LHV)	1.17	0 (i.e., no tar)	[4] [5]
Bubbling Fluidized Bed (BFB)	Direct oxygen blown pressurized	N.A.	N.A.	N.A.	N.A.	1.05	500 mg per Nm^3 of syngas	[8]
Fluidized bed	a) Direct oxygen blown atmospheric; b) Direct oxygen blown pressurized; c) Indirect airblown atmospheric	a) 800; b) 900; c) 900	a) 0.2-0.4 b) 0.2-0.4 c) 0	a) 0.5-2.5 b) 0.5-2.5 c) 1-3	a) 86.0 b) 77.2 c) 65.0	a) 2.18 b) 2.09 c) 2.19	Low (not specified)	[9] [11]
Entrained flow	Indirectly heated	1093	N.A.	N.A.	N.A.	1.0	6.42% of syngas	[7]
Fluidized bed (as implied by the size)	Direct oxygen blown atmospheric	N.A.	N.A.	N.A.	N.A.	N.A.	2 wt.% of the syngas	[10]
Downdraft	Direct oxygen blown atmospheric	N.A.	0.23	0.8-1.2 (finally set at 0.66)	79.5	2.13	N.A. (very low)	[12]

Table 3. Different modelling approaches for the gasifier in gasification-FT studies.

Gasifier modelling	Reference
Syngas temperature and compositions taken from the literature/experiments (empirical data)	[1]
Yield of CH_4 calculated using an equilibrium relation. Yield of heavier hydrocarbons taken from the literature as fixed concentrations. The water–gas shift reaction is assumed to be at equilibrium. No mention about the modelling of the other gasification reactions.	[2]
Combination of Aspen reactor modules and empirical data for a pilot: 1) RYIELD reactor: convert the biomass into fictional components: gaseous H_2, O_2, N_2, H_2O, S, solid C, ash. 2) RGIBBS: calculates a	[3]

product composition at chemical equilibrium. 3) Use of empirical data to adjust the molar fraction of CH_4, C_2H_4 and C_2H_6 and the H_2/CO ratio	
Major gas constituents assumed at thermodynamic equilibrium. Unreacted char wt.%, CH_4 concentration, tar load specified.	[6]
Empirical gasification yield data reconciled (i.e., modified) with biomass composition, oxygen and steam inputs. Elemental mass balance calculations across the gasifier.	[4] [5]
Restricted equilibrium approach (using approach temperatures for reactions). Seven reactions modelled using equilibrium constants.	[4] [5]
Syngas compositions taken from the literature/experiments (empirical data)	[8]
RYIELD reactor followed by RGIBBS. The heat of decomposition from RYIELD is connected to the RGIBBS.	[9] [11]
Stoichiometric reactor model based on the composition of biomass and experimental data on syngas	[7]
Combination of two sections: 1) pyrolysis and oxidation reactions: elemental balance and chemical equilibrium for the water gas shift and methane reactions; 2) char reduction reactions: kinetics-based modelling.	[10]
Syngas compositions taken from the literature/experiments (empirical data)	[12]
RYIELD reactor: convert the biomass and gasifying agents into products using experimental syngas yield and composition	[13]

2.3. Syngas cleaning

The syngas produced by the biomass gasification process contain various contaminants: particulates, condensable tars, BTX (benzene, toluene, and xylenes), H_2S, HCl, NH_3, HCN and COS, alkali compounds, volatile metals. These contaminants can lower activity in the FT synthesis due to catalyst poisoning, therefore deep cleaning is required [1]. When the tars and BTX are removed, the other impurities are removed by standard wet gas cleaning technologies or advanced dry cleaning technologies. Unlike wet syngas cleaning, in dry cleaning the high temperature of the syngas can partly be maintained, but it is still uncertain whether it can meet the high purification requirements of FT synthesis. Indeed, tolerance to contaminants of downstream fuels synthesis is lower compared to the use in combined cycles. The maximum allowed contaminants concentration in syngas for FT synthesis are given in [1] and [2], along with the required treating methods. In summary, the main syngas quality requirements, as reported in [3], are: particle loading in the gas below 0.02 mg/Nm^3; tar loading below 0.1 mg/Nm^3; and sulfur loading below 0.1 mg/Nm^3. The tar removal methods considered in the various studies include thermal cracking at approximately 1300°C, catalytic cracking at 900°C, advanced scrubbing at 400°C using an oil based medium, direct quench water scrubbing.

2.4. Syngas processing

The syngas, produced by the gasification of biomass, consists mainly of H_2, CO, CO_2 and CH_4. Their shares in the syngas can be tailored to the needs of the FT process by methane reforming (converts CH_4 with steam to CO and H_2), a shift reaction (adjusts the H_2/CO ratio by converting CO with steam to H_2 and CO_2) and CO_2 removal [1].

The reforming can be included to maximize the yield of FT fluids. However, in some studies it is not included to minimize the investment costs. Steam methane reforming has been considered in [4] [8] [7] [10]. Instead, the autothermal reforming (ATR) technology has been preferred in [1] [2] [9] [11] and [13]. The reforming/ATR is either applied on the main syngas stream or on the recycle stream returned to the FT reactor.

The water gas shift reactor is included in most studies to increase the hydrogen concentration in the syngas and reach the desired H_2:CO ratio at the inlet of the FT reactor. In only a few studies, see e.g. [9] [12] [1], the optimum H_2:CO ratio can be already achieved by a proper setting of the operating conditions of the gasifier, so that the WGS can be excluded. In [13] the PSA technology is used in place of the WGS reactor.

The CO_2 removal is included in most studies in order to reach a higher C_{5+} selectivity. On the other hand, it might be excluded in the search of lower investment costs. Different CO_2 removal technologies have been considered: amine-based chemical absorption [1] [4], Selexol-based physical absorption [2], Rectisol-based physical absorption [3] [9] [12], membranes [6].

2.5. The FT process

The FT reaction produces hydrocarbons of variable chain length from a gas mixture of carbon monoxide and hydrogen. The main mechanism of the FT reaction is:

$$CO + 2H_2 \leftrightarrow -CH_2- + H_2O \quad (1)$$

The $-CH_2-$ is a building stone for longer hydrocarbons.

- *Selectivity*

A main characteristic regarding the performance of the FT synthesis is the "liquid selectivity" (or C_{5+} selectivity) of the process, which is determined by the "chain growth probability".

The Anderson–Schulz–Flory (ASF) distribution describes the relation between the hydrocarbon yield and the chain growth probability. According to the ASF distribution the molar fraction y of C_n in the hydrocarbon product is:

$$y_{C_n} = \alpha^{n-1}(1-\alpha) \quad (2)$$

where α is chain growth probability and *n* the length of the hydrocarbon.

In terms of weight fractions W the ASF distribution is given by the following equation (Perry's, 2019):

$$log\left(W_{C_n}/n\right) = n \cdot log\alpha + log((1-\alpha)^2/\alpha) \quad (3)$$

Accordingly, different hydrocarbons yields (fuel gas, LPG, naphtha, kerosene, diesel and wax) are obtained for different values of chain growth probability.

A high liquid selectivity is necessary to obtain a maximum amount of long hydrocarbon chains, while reducing to a minimum the yield in the C_1-C_4 range. Selectivity is influenced by several factors including catalysts (iron or cobalt), H_2/CO ratio in the feed gas, temperature, pressure and reactor type [1].

Most of the studies consider a FT product distribution modelling based on the ASF distribution [1] [4] [8] [10] [6] [11]. In [2] this distribution is assumed only in the relevant range of liquid hydrocarbons (C_5-C_{20}), whereas a different distribution is assumed for gaseous hydrocarbons (C_1-C_4). A more advanced triple α model is used in some studies (see e.g. [3]) to overcome the inherent simplifications of a single α model. In some techno-economic analyses [7] [12] the same distribution as that obtained in smaller scale experimental tests was assumed. In most of the studies the chain growth probability α is set to a fixed value in the range 0.8-0.9, [1] [4] [8] [11], where the implicit assumption is that it can be achieved in practice. Then, the liquid selectivity (C_{5+}) is directly calculated from α. Since it is difficult to predict a specific liquid selectivity for biomass derived syngas, three different values of chain growth probabilities have been assumed in [1]. Other authors (see e.g. [2] [10]) calculated α from the liquid selectivity, where the latter was obtained using experimental correlations based on the operational parameters of the FT reactor. Less frequently, like in [6], the α value is calculated using correlations. The products of FT synthesis is often considered limited to linear paraffins (n-alkanes), like in [4] [10] [11]. The products are a mixture of paraffins and olefins in [3] [8]. A more complex product distribution composed of paraffinic hydrocarbons (n-paraffins and isomers), olefins and alcohols was considered in [7], which more closely represent the real product distribution of a FT reactor. At the other end there are studies where the class of products is not even mentioned.

Conversion

In the FT reactor, a high selectivity towards liquid products (longer hydrocarbons) should be combined with a high conversion. The conversion extent in the FT reactor is limited, therefore the reactor product stream contains unreacted carbon monoxide and hydrogen in addition to the FT products. Conversion rate and extent depend especially on availability of reactants and the reactor size, via space velocity (inverse residence time)

and catalyst density. The CO conversion extent is generally set to fixed values depending on the FT reactor technology. Recurrent values are a CO conversion per pass of 40% using mature technology, with the possibility of increasing it by recycling the unconverted syngas. Advanced FT reactors are generally based on once through concepts (i.e., without recycles), with a typical once through conversion of 80%. In the search for a more accurate modelling of CO conversion and for sizing/costing purposes, some authors apply a kinetic-based modelling based on the reaction rates of FT synthesis. This is the approach used in [2], where a once through CO conversion as high as 90% was deemed feasible. The relationship between CO conversion and reactor volume can be clearly seen in [10]. In [12] the data on CO conversion are directly taken from the lab scale experiments and simply correlated with the space velocity. To increase CO conversion while using established FT technology gas recycle is employed. Here various configurations are considered, where the gas is simply recycled to the inlet of the FT reactor [1], to the syngas cleaning area [4], to the reforming reactor [2] [7] [9] [11], or even recycled back to the gasifier [2] [6] [10].

Table 4. Modelling and operating conditions of the FT reactor in gasification-FT studies in the literature.

Conversion modelling	Conversion extent	FT product distribution modelling	Chain growth probability (α)	Liquid selectivity (C_{5+})	Product categories	Reference
Fixed values	a) CO conversion per pass 40% (possible recycle); b) Once through conversion: 60-80%	ASF distribution (i.e., single α model)	0.8-0.9	Calculated from α: 73.7-91.9%	Not mentioned	[1]
Calculated from the reaction rate for a given reactor size (kinetic-based modelling)	a) CO conversion per pass 70% (possible recycle); b) Once through conversion: 70-90%	ASF distribution (only in the relevant range of C_5-C_{20})	Calculated from selectivity C_{5+}	Relation with T, p, $[H_2]$ and [CO] in the feed gas	Not mentioned	[2]
Fixed value	Once through conversion: 80%	Triple α model	N.A.	N.A.	Mixture of straight-chain hydrocarbons: paraffins (C_nH_{2n+2}) and olefins (C_nH_{2n})	[3]
Fixed values	CO conversion: 40-60-80%	ASF distribution	Calculated from the partial pressures of CO and H_2, rate constant for the adsorption of CO, rate constant for desorption of paraffins and olefins	N.A. (Calculated from α)	N.A.	[6]
Fixed value	a) CO conversion per pass 40% (possible recycle);	ASF distribution	0.90	N.A. (Calculated from α)	Linear paraffins (i.e., n-alkanes)	[4] [13]
Fixed value	CO conversion: 75%	Liquid hydrocarbons follow the same distribution as obtained in the experimental tests by the same authors	N.A.	74.4%	Paraffinic hydrocarbons (N-paraffins and isomers), olefins and alcohols	[7]

Isothermal plug flow reactor with varying length (kinetic-based modelling)	Once through conversion: 80%	ASF distribution	0.85	N.A. (Calculated from α)	Alkanes and alkenes from C_1 to C_{20}	[8]
Fixed values	a) CO conversion per pass 40% (possible recycle); b) Once through conversion: 80%	Equal distribution between the four product types (light gases, naphtha, diesel and waxes)	0.90 (implied)	75% (implied)	Three long-chained alkanes: C_9H_{20} for gasoline, $C_{15}H_{32}$ for diesel and $C_{21}H_{44}$ for waxes	[9]
Calculated from the reaction rate for a given reactor size (kinetic-based modelling)	Variable depending on off-gas recycle and FT reactor volume	ASF distribution	Calculated from selectivity C_{5+} (α=0.73)	Relation with T, p, $[H_2]$ and [CO] in the feed gas	Linear paraffins (i.e., n-alkanes)	[10]
Fixed value	CO conversion per pass 40% (possible recycle)	ASF distribution	0.89	N.A. (Calculated from α)	Linear paraffins (i.e., n-alkanes)	[11]
From the lab scale experiments	Variable in the range 43-73% depending on space velocity (i.e., reactor volume)	Same distribution as obtained in the experimental tests	Evaluated in the C_{10}-C_{24} range from experiments (α=0.89-0.96)	N.A.	N.A.	[12] (Ail & Dasappa, 2016)

2.6. Hydrocracking and product separation

When diesel or kerosene are the desired final products, the FT product requires hydrocracking. Hydrocracking involves the breaking up of the large hydrocarbon molecules in the waxy product into desired final products in a hydrogen-rich environment. Hydrogen is added to remove double bonds (saturating the olefins), after which the FT-liquids are cracked catalytically with hydrogen. Depending on the hydrocracking conditions, mainly diesel or kerosene are produced, with a smaller percentage fraction of naphtha. First, the C_{5-9} fraction is separated from the heavier products. The waxy part C_{10+} of the raw synthesis product is selectively hydrocracked to the desired middle distillate products C_{10-20}. Simultaneously, the product is isomerized to improve the cold flow properties, and subsequently fractionated in a conventional distillation column.

2.7. Use of the off-gas

After the FT synthesis cooling to 50°C makes it possible for the C_{5+} fraction to be separated as liquid. The off-gas, which is formed by the C_1–C_4 fraction, can be used either in a thermal engine (piston engine, gas turbine) for electricity production or to produce additional fuels or chemicals. Due to the large scale considered in many studies, the preferred technology for utilization of the off-gas is based on the gas-steam combined cycle [3] [4], [9], possibly in co-firing with natural gas [1]. In several studies [8] [6] [11] the off-gas is burnt in a boiler for the production of high pressure steam and power generation in a steam power cycle. In the smaller scale system of [12] the off-gas is used in a boiler for the generation of steam required by gasification and in an internal combustion engine for power production. In [10] additional power was obtained by expansion of the high pressure off-gas in a turbine. A different utilization route of off-gas is proposed in [13], where useful chemical/fuels are produced rather than power. In particular, propane is separated using cryogenic distillation, whereas hydrogen is separated using PSA.

2.8. Characteristics of the FT products

The FT products are totally free of sulphur, nitrogen, nickel, vanadium, asphaltenes, and aromatics which all are typically found in mineral oil products.

FT-diesel has a very high cetane number, which is a primary measure of diesel fuel quality. On the other hand, the FT naphtha has a much lower octane number than normal naphtha, which implies a low quality of the FT-

gasoline. The product upgrading area considered in [3] includes a naphtha hydrotreater followed by an isomerization unit. The latter increases the octane number of the pentane/hexane stream produced by the naphtha hydrotreater, producing high-grade gasoline blending component. FT-kerosene has been ASTM approved.

In most of the studies the only desired FT product is FT-Diesel [1] [2] [8] [10]. In other papers, there is interest also in the co-product FT-Gasoline [3] [4] [7]. The more generic FT liquid products or FT syncrude represent the desired output in [6], [9], [12], without any information about the application. Only few studies specifically target the production of jet fuel [11] [13]. The chemical composition of the specific FT product (gasoline, diesel, jet fuel) is generally not shown in the techno-economic analyses, which simply characterize the FT product in terms of range in carbon atoms number. Only in [13] the physical properties of the FT jet fuel are shown as predicted by Aspen. In particular, the values of density, viscosity, freezing point, flash point and heating value are shown and compared against those of fossil jet fuel (Jet A).

3. The RWGS-Fischer Tropsch route for the production of e-kerosene

This section deals with the critical analysis of the techno-economic studies addressing the production of e-kerosene. The focus is on the modelling approach used for the simulation of the reverse water gas shift reactor (RWGS) and for the FT synthesis.

3.1 The reverse water gas shift reactor

The Reverse Water-Gas Shift (RWGS) reaction is a chemical reaction in which the conversion of hydrogen (H_2) and carbon-dioxide (CO_2) into Carbon-monoxide (CO) and water (H_2O) occurs. There are several types of reactors that can be used for the RWGS reaction. The most common RWGS reactor is Fixed-bed reactor in which the fixed catalyst bed is used. The reaction takes place on the surface of catalyst when the reactant gases pass through the catalyst fixed on bed. Reverse Water Gas Shift reaction is an equilibrium as well as an endothermic reaction that is thermodynamically favoured by elevated-temperatures:

$$CO_2 + H_2 \rightarrow CO + H_2O \quad (4)$$

The FT reaction typically occurs at high pressure (20-40 bar), so it is recommended to operate within this pressure range for the RWGS reaction as well, considering pressure drops in the equipment. In fact, the best and the most efficient way is to compress the working fluids before the RWGS reaction rather than compressing it between the reactors. This approach reduces energy and economic expenses associated with cooling and heating the gases, as well as issues arising from water formation in the products. However, there are certain drawbacks, such as the high construction and material cost and undesired side reactions leading to coke formation and methane, as shown below:

$$CO_2 + 4H_2 \rightarrow CH_4 + 2H_2O \quad (5)$$

$$CO + 3H_2 \rightarrow CH_4 + H_2O \quad (6)$$

$$CO_2 + 2H_2 \rightarrow C_{(s)} + 2H_2O \quad (7)$$

$$2CO \rightarrow C_{(s)} + CO_2 \quad (8)$$

To promote the RWGS reaction and maximize CO production, operational conditions should favor high temperatures. Methane and Coke, which are undesired products, are stable at temperatures below 700 and 900°C, respectively. Operating at temperatures above 700°C helps minimize CH_4 formation and increase the CO fraction. Additionally, working with a high H_2/CO_2 ratio reduces formation of coke and enhances the CO_2 conversion into CO. Table 5 shows the operating conditions and modelling approaches considered in the literature for the RWGS reactor.

Table 5. Operating conditions and modelling approaches used in the literature for the RWGS reactor.

H_2/CO_2 molar ratio	T (°C)	P(bar)	Modelling	Reactions	Reference
3.0	800	30	Equilibrium conversion using REquil reactor	RWGS only (100% selectivity to CO)	[15]
Variable around 2.0 to provide a constant molar ratio of $H_2/CO = 2$ in the feed of the FT reactor	550-950	1-25	Equilibrium conversion using RGibbs reactor	RWGS and side reactions involving methane (carbon is not included)	[16]
1.0	600	24.5	Stoichiometric reactor using fixed conversion based on the experimental results: CO_2 conversion ratio of 36%	RWGS only	[17]
3	800-860	30	Kinetics based: plug flow reactor, adiabatic	RWGS, CO_2 methanation, CO methanation	[14]

3.2. The FT reactor in the production of e-kerosene

As for the FT reactor fed by the RWGS syngas, different modelling approaches have been used, as shown in Table 6.

Table 6. Operating conditions and modelling approaches of FT synthesis reactor.

Reactor	H_2/CO in syngas feed	Chain growth reactions	CO conversion (%)	Modelling	Chain growth probability α	FT products	Reference
Stoichiometric reactor RStoic	/	Combined CO and CO_2 hydrogenation (eight reactions)	/	Per-pass yield of each chain growth reaction is specified, according to the Fe-based FTS experimental data	/	Only four hydrocarbons: CH_4, C_3H_8, $C_{12}H_{26}$ (paraffins); C_3H_6 (olefins)	[15]
Stoichiometric reactor RStoic	2	CO hydrogenation	40	ASF distribution but fixed methane selectivity	0.839 (calculated)	Only alkanes (C_1-C_{30}, C_{32}, C_{36})	[16]
Stoichiometric RStoic	2.2	CO hydrogenation	52.2	ASF distribution	0.9	Only alkanes (C_1-C_{20}, C_{30})	[17]
Kinetics based: plug flow reactor, isothermal	2	Paraffins, olefins and WGS reactions	Calculated from the kinetic model	ASF distribution. Kinetic model with an explicit dependence on α parameter	N.A.	Only paraffins up to C_{30}	[14]

4. Modelling and simulation of the Gasification-Fischer Tropsch route

This section addresses the modelling of the biomass gasifier and the FT reactor used in the G-FT route for the production of bio-kerosene. The simulation results for both sections are shown.

4.1. Modelling the biomass gasification

Figure 1 shows the flowsheet of the biomass gasification section developed in Aspen Plus. In the yield reactor ("RYIELD") the biomass is decomposed into its constituting components, including carbon, hydrogen, oxygen, nitrogen, sulfur, chlorine and ash. The yield distribution is specified from the biomass ultimate analysis, entered as component attribute, by using a calculator block. In the reactor "RGIBBS" a Gibbs free energy minimization is done to determine the product composition at chemical equilibrium. Oxygen and steam are used as the gasifying agents of the atmospheric gasifier. The two reactors are connected by a heat stream, to account for the heat of decomposition. Since the formation of tar cannot be assessed by chemical equilibrium, the tar yield is set on the basis of experimental data in RYIELD, and it is considered inert in RGIBBS. In the solid separator (SSEP) the gas is separated from the solids, namely ash and, in case of incomplete conversion, also char. After cooling to approximately the ambient temperature the syngas is

separated from the liquid (mainly water). More accurate biomass gasification models that include reaction kinetics for char gasification have been developed in the literature (see e.g. Puig-Arnavat, 2010). On the other hand, the chemical equilibrium approach has been preferred in this work and used as a theoretical benchmark. This is also consistent with the modelling approach used in several studies in the literature (see Table 3).

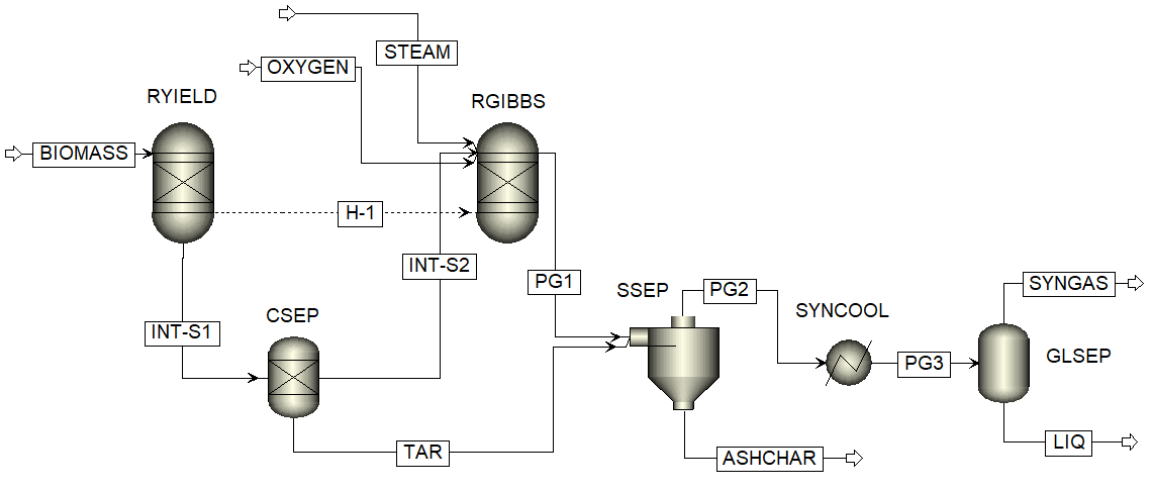

Figure 1. Aspen flowsheet of the biomass gasification section.

The Aspen model was run using Casuarina wood chips as the feedstock, taking advantage of the experimental data available in [18] and [12] for oxy-steam gasification of such tropical wood. Due to some missing properties and inconsistencies, the Casuarina wood properties were taken from the open source database Phyllis, and are shown in Table 7. It is assumed that the wood chips are dried at around 100°C, bringing their moisture content to only 1%. The proximate and ultimate analyses (Table 7) are entered as attributes of the biomass nonconventional component. The net and gross caloric values as given in Phyllis (Table 8) are used as input parameters, instead of calculating them by the coal enthalpy model "HCOALGEN".

Table 7. Ultimate and proximate analyses of the biomass feedstock (Casuarina wood chips).

Ultimate analysis	wt%	Proximate analysis	wt%
Carbon	48.80	Moisture content	1
Hydrogen	5.83	Ash content	1.40
Oxygen	43.36	Volatile matter	78.94
Nitrogen	0.59	Fixed carbon	19.66
Sulfur	0.02	Total (dry basis)	100
Chlorine	≈0		
Ash	1.40		
Total (dry basis)	100		

Table 8. Lower and higher heating values of the biomass feedstock (Casuarina wood chips).

Heating values	Wet basis	Dry basis	Dry ash free
Net calorific value, LHV (MJ/kg)	17.96	18.17	18.43
Gross calorific value, HHV (MJ/kg)	19.25	19.44	19.72

4.2. Simulation results for the gasifier

The simulation model has been validated against the experimental results presented in [18] and [12] for particular operational conditions of the gasifier. After validation, the simulation model has been run in a wide range of oxygen-to-biomass (OBR) and steam-to-biomass ratios (SBR), to identify the optimum gasification parameters. Table 9 shows the syngas composition obtained for a specific operational condition, which was selected in [12] as the most suitable for a gasification-FT system.

Table 9. Syngas composition: comparison between experimental results and simulation results for OBR=0.23 and SBR=0.66.

Syngas composition	Experimental results [12]	Aspen simulation
y_{H2} (%)	47±2	50.4
y_{CO} (%)	22±3	24.4
y_{CO2} (%)	27±1.6	21.5
y_{CH4} (%)	4±0.5	1.2
y_{H2O} (%)	N.A. or dry basis	2.3
H_2:CO ratio	2.14	2.07
Temperature (°C)	N.A.	680

The chemical equilibrium model developed in Aspen predicts a higher concentration of hydrogen and a lower concentration of methane compared to the experimental results, which is consistent with the findings of [18]. Overall, the predicted H_2:CO ratio is very similar. The gasifier operational condition used for model validation is superposed as a red mark in Figure 2, where contour plots of H_2:CO ratio, gasifier temperature and gasifier efficiency are shown as a function of OBR and SBR. While these plots have been obtained using the chemical equilibrium assumption, yet they show interesting trends. High H_2 to CO molar ratios are obtained in the upper left corner, which is characterized by SBR>0.6 and OBR<0.28. In this region the syngas temperature is moderate, in the range 650-800°C. Two definitions of gasifier efficiency have been considered. The "cold gas efficiency" (LHV based) is the ratio between the energy content of syngas and the energy content of biomass:

$$CGE = \frac{\dot{m}_{syn} LHV_{syn}}{\dot{m}_{biom} LHV_{biom}} \tag{9}$$

The second definition, here called generally gasification efficiency (η_g), takes into account also the energy input for steam generation, according to:

$$\eta_g = \frac{\dot{m}_{syn} LHV_{syn}}{\dot{m}_{biom} LHV_{biom} + \dot{Q}_{steam}} \tag{10}$$

The highest values of CGE (Figure 2c) are obtained at the upper left corner, which are also associated with favorable conditions in terms of H_2:CO ratios. At low OBR and SBR the CGE drops mainly due to the incomplete carbon conversion and residual char formation. When the energy demand for steam generation is taken into account, the gasification efficiency (Figure 2d) drops and the region of maximum moves towards the use of oxygen as the only gasifying agent. However, this region is unsuitable in terms of H_2:CO ratios for the FT reaction.

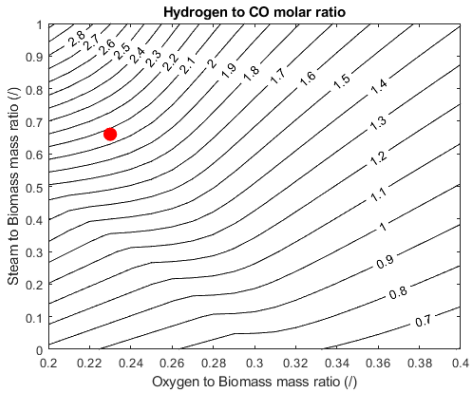

a)

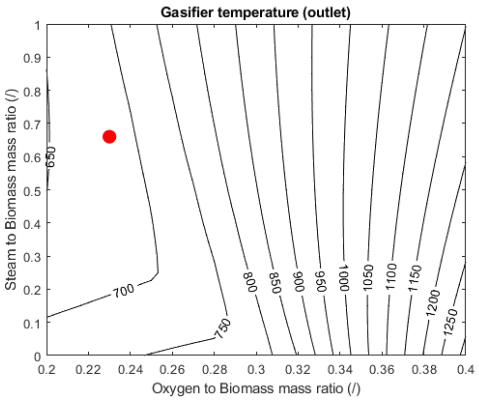

b)

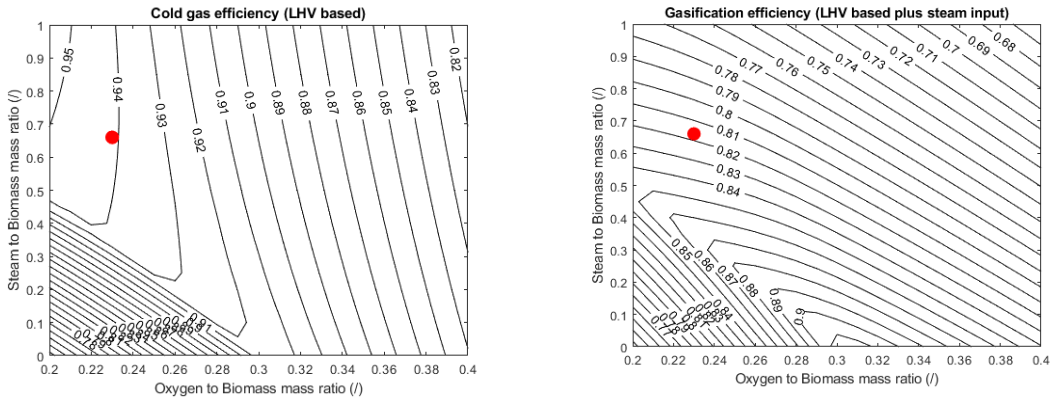

c) d)

Figure 2. Variation of the gasifier parameters as a function of the oxygen to biomass mass ratio (OBR) and steam to biomass mass ratio (SBR): a) H_2:CO ratio; b) gasifier temperature at the outlet; c) cold gas efficiency (LHV based); d) gasification efficiency (LHV based plus steam input).

Table 10. Syngas composition for the selected operating condition OBR=0.23 and SBR=0.66.

Syngas composition	Mole flow (kmol/hr)	Mole fraction (%)	Mass flow (kg/hr)	Mass fraction (%)
CO	206.0	24.40	5770.8	37.99
H_2	425.1	50.35	857.0	5.64
CO_2	181.6	21.51	7992.6	52.62
CH_4	9.8	1.16	157.1	1.03
H_2O	19.6	2.32	352.9	2.32
N_2	2.1	0.24	57.7	0.38
H_2S	0.06	0.007	2.1	0.014
NH_3	0.01	0.001	0.16	0.001
Total	844.3	100	15190	100

4.3. Modelling the FT reactor

The FT reactor has been modelled in Aspen Plus as a stoichiometric reactor "RSTOIC" (Fig. 3). It is assumed that the reactor is fed with clean syngas with a level of contaminants lower than the specifications for cobalt FT synthesis. Due to the favourable H_2:CO ratio of the syngas produced by the gasifier and the low concentration of methane, the syngas conditioning would include only a CO_2 removal unit.

Table 11. Syngas feed to the FT reactor.

Component	Mole flow (kmol/hr)	Mole fraction (%)	Mass flow (kg/hr)	Mass fraction (%)
CO	206.0	32.56	5770	87.03
H_2	426.6	67.44	860	12.97

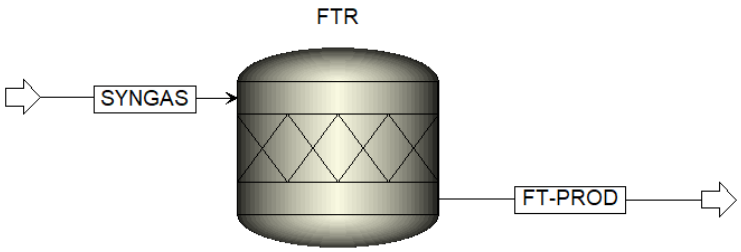

Figure 3. The stoichiometric reactor unit used for the modelling of the FT reactor.

The temperatures of the FT reactor was set at 230°C and the pressure at 30 bar, which are typical of low temperature FT and consistent with [12]. All the stoichiometric reactions for the synthesis of n-paraffins, from C_1 to C_{20} plus the reaction for C30 were entered in the form:

$$(2n+1)H_2 + nCO \rightarrow C_nH_{2n+2} + nH_2O \tag{11}$$

It is known that the "reaction coordinate" (also called degree or extent of reaction) characterizes the extent or degree to which a reaction has taken place. It is defined by the following equation:

$$dn_i = \nu_i d\varepsilon \quad (i = 1,2,\dots,N) \tag{12}$$

where dn_i is the differential change in the number of moles of species *i* and ν_i is the stoichiometric number.

In multireaction stoichiometry [19], where more independent reactions proceed simultaneously, a separate reaction coordinate (ε_j) applies to each reaction *j*. Because the number of moles of a species n_i may change because of several reactions, the general equation analogous to Eq. 12 includes a sum:

$$dn_i = \sum_j \nu_{i,j} d\varepsilon_j \quad (i = 1,2,\dots,N) \tag{13}$$

where $\nu_{i,j}$ designates the stoichiometric number of species *i* in reaction *j*.

Integration from $n_i = n_{i0}$ and $\varepsilon_j = 0$ to arbitrary n_i and ε_j gives:

$$n_i = n_{i0} + \sum_j \nu_{i,j}\varepsilon_j \quad (i = 1,2,\dots,N) \tag{14}$$

Summing over all the hydrocarbon species formed in the FT reactor yields:

$$n_{HCs} = \sum_i n_i \tag{15}$$

And by definition the molar fraction of each hydrocarbon species in the hydrocarbon product is:

$$y_i = \frac{n_i}{n_{HCs}} \quad (i = 1,2,\dots,N) \tag{16}$$

Since the molar fraction of each hydrocarbon (n-paraffin) species is known from the ASF distribution, the problem is a reverse problem, because it consists in determining the reaction coordinate of each reaction ε_j from the known values y_i. The solution can be addressed in terms of either fractional conversion or reaction extent, as explained in Appendix A.

In this work the molar extent of each reaction was specified in Aspen by the calculated values of fractional conversion using a calculator block, following the approach described in [5]. Two values of overall CO conversion have been considered equal to 40% and 80%, as representative of a standard and advanced FT reactor, respectively. In both cases the chain growth probability has been assumed equal to α=0.9. The implicit assumption is that these values can be achieved by a proper choice of the reaction conditions and the catalysts.

4.4. Simulation results for the FT reactor

Figure 4 shows the molar fraction and mass fraction of FT products (n-paraffins) obtained from the simulation model. It clearly appears that the FT products follow the ASF distribution for hydrocarbons in the carbon atom

range C_1-C_{20}. Instead, to limit the number of species in the Aspen model, the mass/molar fractions of longer hydrocarbons are lumped together in a single hydrocarbon ($C_{30}H_{62}$), which is taken as representative of the heavier FT fraction (wax).

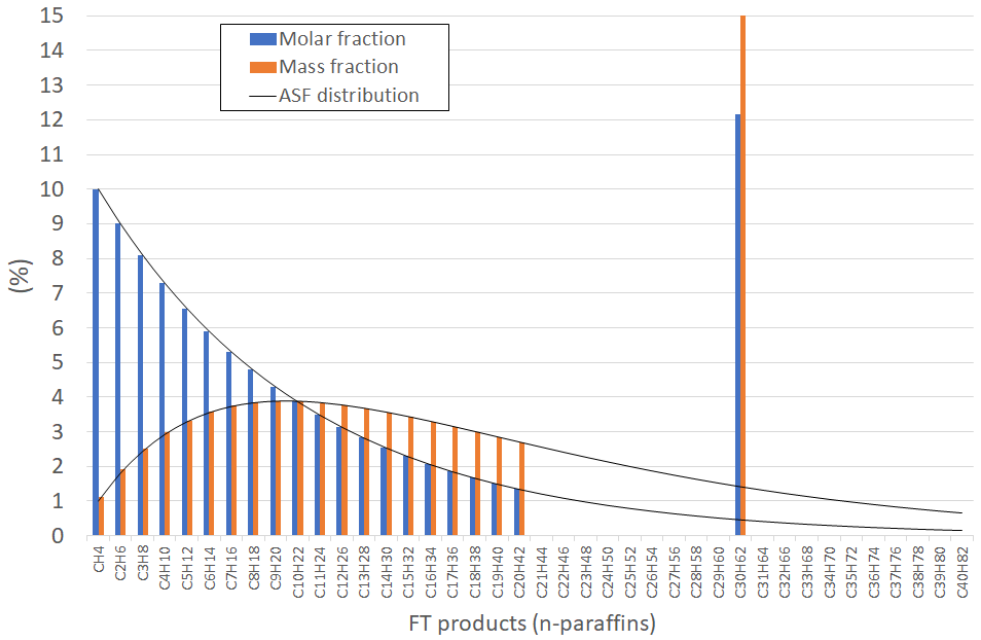

Figure 4. Molar fractions (blue bars) and mass fractions (orange bars) of FT products obtained from the Aspen model. The theoretical ASF distribution is superposed as a solid line on the bar charts.

Table 12 shows the composition and flow rate of the product leaving the FT reactor under the two scenarios considered. The C_{5+} hydrocarbons are grouped in four categories, namely gasoline, jet fuel, diesel and wax depending on the number of carbon atoms.

Table 12. Composition and flow rate of the product stream of the FT reactor for a CO conversion=0.4.

Species	Mole fraction (%)	Mole flow rate (kmol/hr)	Mass fraction (%)	Mass flow rate (kg/hr)
H_2	54.20	253.58	7.71	511.2
CO	26.42	123.60	52.22	3462.0
CH_4	0.18	0.824	0.20	13.2
C_2H_6	0.16	0.742	0.34	22.3
C_3H_8	0.14	0.667	0.44	29.4
C_4H_{10}	0.13	0.601	0.53	34.9
C5-C7 (gasoline)	0.31	1.465	1.88	124.8
C8-C16 (jet fuel)	0.52	2.414	5.85	387.8
C17-C20 (diesel)	0.11	0.525	2.06	136.4
C30 (wax)	0.21	1.002	6.39	423.6
H_2O	17.61	82.40	22.38	1484.4
Total	100	467.81	100	6630

When the CO conversion is increased to 0.8 the flow rates of hydrocarbons double compared to the values shown in Table 12. Accordingly, the mass flow rate of jet fuel would reach around 775 kg/hr. The properties of the liquid hydrocarbon mixture (C_8-C_{16}) composing jet fuel have been calculated using Aspen Plus. It can be seen from Table 13 that the obtained jet fuel falls short of Jet-A1 in several properties due to its composition.

Table 13. Estimated properties of the FT jet fuel as compared to Jet-A1.

Properties	FT jet fuel properties	Jet-A1 (ASTM D7566)
Density at 15°C (kg/m^3)	731.6	775-840
HHV (MJ/kg)	37.13	42.80 (min)
LHV (MJ/kg)	33.76	/

Kinematic viscosity at -20°C	4.43	8 (max)
Flash point (°C)	30.0	38 (min)
Freezing point (°C)	N.A.	-47 (max)

5. Modelling and simulation of the RWGS-Fischer Tropsch route

This section addresses the modelling and simulation of the syngas production in the RWGS reactor, which is used for the production of e-kerosene. It is assumed that the syngas obtained is converted in a FT synthesis reactor using the same modelling approach as that used for conversion of the bio-syngas.

5.1. Modelling of the RWGS reactor

Figure 5 shows the schematic of the Aspen simulation model developed for the RWGS section. Hydrogen and CO_2 are compressed to the target pressure, mixed and heated to the desired temperature of the RWGS reactor. A Gibbs reactor (RGIBBS) was used to calculate the chemical equilibrium of the reverse water shift reaction as well as of the side reactions. The produced syngas is cooled to 40°C to separate water as condensate.

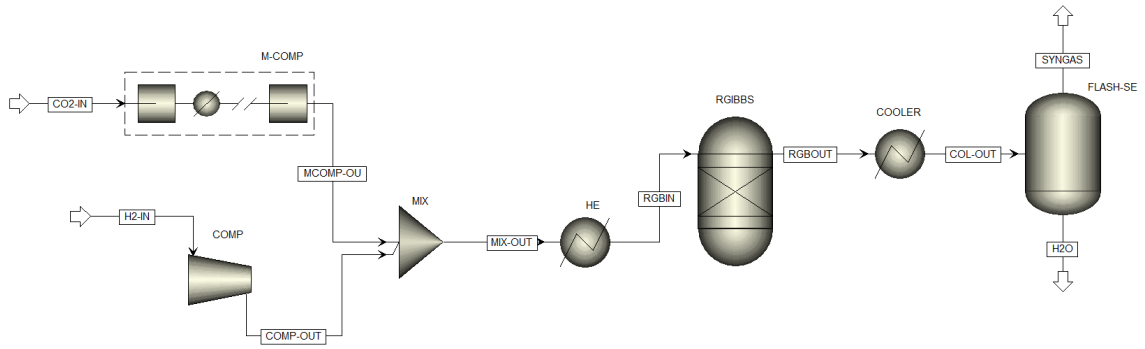

Figure 5. Aspen flowsheet of the syngas generation section from hydrogen and CO_2 using the RWGS reactor.

5.2. Results obtained for the RWGS reactor

The RWGS simulation model was run in a wide range of reactor pressures (10-30 bar) and temperatures (700-950°C) for a fixed H_2:CO_2 molar ratio of the feed stream equal to 2. The aim is to explore the best conditions for the operation of the RWGS, while considering the requirements of the downstream FT unit.

The following parameters were calculated:

i) The H_2:CO molar ratio (Fig. 6a), to verify whether suitable conditions can be obtained for the following FT reactor, which requires H_2:CO ≈ 2.1.

ii) The CO yield (Fig. 6b), which is defined by the ratio between the molar flowrate of CO leaving the reactor and the molar flowrate of CO_2 entering the reactor:

$$Y_{CO} = \frac{\dot{n}_{CO,out}}{\dot{n}_{CO_2,in}} \tag{17}$$

iii) The methane yield (Fig. 6c), which is defined by the ratio between the molar flowrate of CH_4 leaving the reactor and the molar flowrate of CO_2 entering the reactor:

$$Y_{CH_4} = \frac{\dot{n}_{CH_4,out}}{\dot{n}_{CO_2,in}} \tag{18}$$

iv) The CO selectivity (Fig. 6d), which is defined by the ratio between the molar flowrate of CO leaving the reactor and the molar flowrate of CO_2 that reacted:

$$S_{CO} = \frac{\dot{n}_{CO,out}}{\dot{n}_{CO_2,in} - \dot{n}_{CO_2,out}} \tag{19}$$

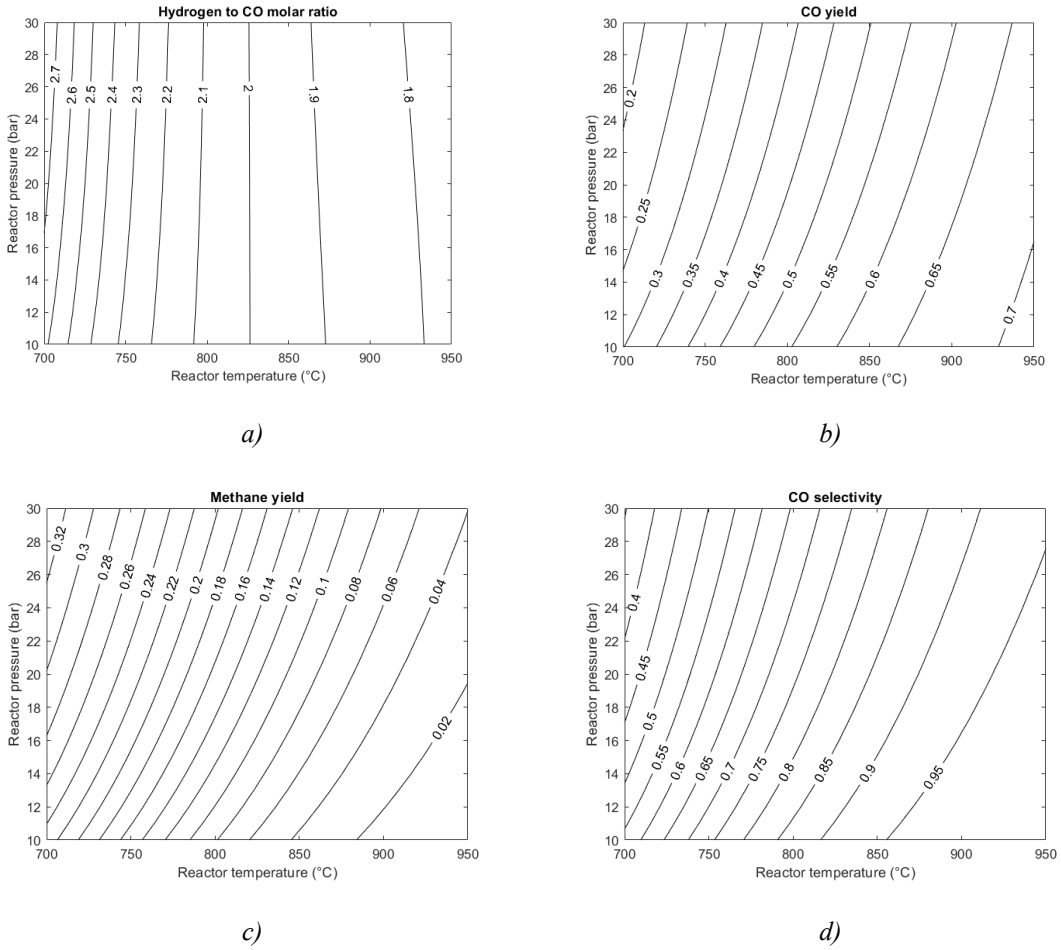

Figure 6. Variation of the parameters of the RWGS reactor as a function of the reactor temperature and reactor pressure: H_2 to CO molar ratio, CO yield, methane yield and CO selectivity.

From the analysis of the response surfaces shown in Fig. 6, it appears that the CO yield increases as the reactor temperature increases and the pressure decreases. The CO yield is lower than one due to the equilibrium conversion and the side CO_x methanation reactions. The methane yield is significant at reactor temperatures lower than 850°C and pressures higher than 10 bar. At the highest pressures values of CO selectivity higher than 90% require reactor temperatures higher than 900°C. According to the trends shown in Fig. 6, an operation point was selected that ensures the proper H_2:CO ratio and a satisfactory performance in terms of CO yield and selectivity. The underlying assumption is that the CO_2 fraction and the CH_4 fraction in the syngas does not affect the operation of the downstream FT reactor. The syngas flow rates and compositions are shown in Table 14.

Table 14. Syngas parameters obtained assuming a reactor temperature of 850°C, a pressure of 30 bar and a hydrogen to CO_2 ratio equal to 2 in the feed.

Syngas composition	Mole flow (kmol/hr)	Mole fraction (%)	Mass flow (kg/hr)	Mass fraction (%)
CO_2	181.4	22.80	7982.9	53.57
H_2	353.9	44.48	713.3	4.79
CO	169.2	21.27	4740.5	31.81

CH_4	89.2	11.21	1431.4	9.61
H_2O	1.9	0.24	33.8	0.23
Total	795.6	100	14901.9	100

Using the same approach as that used for the bio-syngas, the FT reactor model was run using only the CO and H_2 flowrates as gas feed. Similarly to the bio-syngas case, two values of CO conversion, namely 40% and 80%, were assumed and the chain growth probability α was kept equal to 0.9. Assuming a CO conversion of 40% the mass flow rate of jet fuel is 318.6 kg/hr, whereas with a CO conversion of 80% the mass flow rate of jet fuel would reach 637.2 kg/hr.

6. Preliminary comparison between the performance of the two routes

Table 15 shows the results obtained from a preliminary comparison between the two pathways for the production of jet fuel. It is assumed the that the energy input is the biomass feedstock in the bio-jet fuel scenario, whereas the energy input is associated with hydrogen only in the e-jet fuel scenario. The heating value of the jet fuel obtained (assumed in both routes to be equal to a blend of n-alkanes with carbon atom length in the range C_8-C_{16}) was calculated in Table 13.

Table 15. Jet fuel yield and energy efficiency in the production of biojet fuel and e-jet fuel.

Product	Mass flow rate feed (kg/hr)	Energy input (HHV basis)	Mass flow rate jet fuel (kg/hr)	Energy jet fuel (HHV basis)	Efficiency (%)
Bio-jet fuel	10000 (biomass)	54.0	387.8-775	4.0-8.0	7.41-14.80
E-jet fuel	715 (hydrogen)	28.2	318.6-637.2	3.3-6.6	11.66-23.32

Conclusions

Two production routes have been considered in this work for the production of sustainable aviation fuels: the bio-jet fuel route is based on biomass gasification and Fischer-Tropsch synthesis; the e-kerosene route is based on syngas production from green hydrogen and captured CO_2, which is followed, also in this case, by the FT synthesis. By conducting a critical review of the techno-economic studies in the literature and through the modelling of the main processes in these two routes, it has been shown that suitable feed conditions for the FT reactor can be directly obtained in a wide range of the operational parameters of the gasifier as well as of the reverse water gas shift reactor. However, it is possible to combine a high gasification efficiency with the desired H_2:CO molar ratio for the FT reactor only by properly selecting the oxygen/steam to biomass ratios in a narrower range. Similarly for the RWGS, it is possible to combine a high CO yield and CO selectivity with the required FT reactor feed conditions by properly choosing the reactor pressure and temperature.

The single modeling approach used for the FT reactor for both routes implies the same composition and properties of the jet fuel obtained, which still falls short the Jet-A fuel properties. On the other hand, the refining processes with hydrogen following the FT reactor would allow to reach the aviation fuel specifications and to further increase the jet fuel yield. The preliminary jet fuel yields and energy efficiency estimates based on the heating values show a superiority of the e-kerosene pathway, which however uses hydrogen as feedstock and assumes a readily available CO_2 source. The lower energy efficiency of the bio-jet pathway (estimated approximately equal to 15%) would largely be compensated by using a waste biomass as feedstock. In this context, the technological advancements in applying the FT technology for conversion of biomass derived syngas containing impurities, rather than a clean syngas, appear fundamental.

The analysis of these two routes under the same framework would allow the exploitation of the research findings in both these fields, which currently often proceed in parallel, with obvious advantages in terms of resources utilization and more opportunities of implementation.

Appendix A

A.1 Solution in terms of reaction extent

Equation (4) can be written for each of the hydrocarbon products considering that $n_{i0} = 0$ and that all the stoichiometric coefficients of hydrocarbons are equal to 1 (see Eq. 1). Accordingly, the number of moles of hydrocarbon species i formed in reaction j is equal to the reaction coordinate ε_j:

$n_{CH_4} = \varepsilon_1, n_{C_2H_6} = \varepsilon_2, n_{C_3H_8} = \varepsilon_3, \ldots, n_{C_{20}H_{42}} = \varepsilon_{20}, n_{C_{30}H_{62}} = \varepsilon_{30}$

Summing over all hydrocarbon products:

$n_{HCs} = \varepsilon_1 + \varepsilon_2 + \varepsilon_3 + \cdots + \varepsilon_{20} + \varepsilon_{30}$

By the definition of molar fraction:

$$y_{CH_4} = \frac{n_{CH_4}}{n_{HCs}} = \frac{\varepsilon_1}{\varepsilon_1 + \varepsilon_2 + \varepsilon_3 + \cdots + \varepsilon_{20} + \varepsilon_{30}} = \frac{\varepsilon_1}{n_{HCs}}$$

$$y_{C_2H_6} = \frac{n_{C_2H_6}}{n_{HCs}} = \frac{\varepsilon_2}{n_{HCs}}$$

$$y_{C_3H_8} = \frac{n_{C_3H_8}}{n_{HCs}} = \frac{\varepsilon_3}{n_{HCs}}$$

…

$$y_{C_{20}H_{42}} = \frac{n_{C_{20}H_{42}}}{n_{HCs}} = \frac{\varepsilon_{20}}{n_{HCs}}$$

$$y_{C_{30}H_{62}} = \frac{n_{C_{30}H_{62}}}{n_{HCs}} = \frac{\varepsilon_{30}}{n_{HCs}}$$

All these mole fractions can also be calculated as a function of the carbon number and alpha by the ASF distribution.

By writing Eq. 4 for the CO species and assuming that $n_{CO,0}$ is the fraction of CO feed that reacts in the FT reactor, and the after reaction completion $n_{CO} = 0$, we obtain:

$\varepsilon_1 + 2 \cdot \varepsilon_2 + 3 \cdot \varepsilon_3 + \ldots + 20 \cdot \varepsilon_{20} + 30 \cdot \varepsilon_{30} = n_{CO,0}$

The system of equations can be solved in $\varepsilon_1, \varepsilon_2, \varepsilon_3, \ldots, \varepsilon_{20}, \varepsilon_{30}$ and n_{HCs}.

A.2 Solution in terms of fractional conversion

By using the definition of fractional conversion and from Eq. (4) written for the CO species:

$$\chi_{CO_{R1}} = \frac{n_{CO,0} - n_{CO,R1}}{n_{CO,0}} = \frac{\varepsilon_1}{n_{CO,0}}$$

$$\chi_{CO_{R2}} = \frac{n_{CO,0} - n_{CO,R2}}{n_{CO,0}} = \frac{2 \cdot \varepsilon_2}{n_{CO,0}}$$

$$\chi_{CO_{R3}} = \frac{n_{CO,0} - n_{CO,R3}}{n_{CO,0}} = \frac{3 \cdot \varepsilon_3}{n_{CO,0}}$$

…

$$\chi_{CO_{R20}} = \frac{n_{CO,0} - n_{CO,R20}}{n_{CO,0}} = \frac{20 \cdot \varepsilon_{20}}{n_{CO,0}}$$

$$\chi_{CO_{R30}} = \frac{n_{CO,0} - n_{CO,R30}}{n_{CO,0}} = \frac{30 \cdot \varepsilon_{30}}{n_{CO,0}}$$

Considering that:

$n_{HCs} = \varepsilon_1 + \varepsilon_2 + \varepsilon_3 + \cdots + \varepsilon_{20} + \varepsilon_{30}$

And using the above expressions of fractional conversion:

$$n_{HCs} = n_{CO,0} \cdot \left(\chi_{CO_{R1}} + \frac{\chi_{CO_{R2}}}{2} + \frac{\chi_{CO_{R3}}}{3} + \cdots + \frac{\chi_{CO_{R20}}}{20} + \frac{\chi_{CO_{R30}}}{30}\right)$$

The mole fractions can be expressed as a function of the fractional conversions:

$$y_{CH_4} = \frac{n_{CH_4}}{n_{HCs}} = \frac{\chi_{CO_{R1}}}{\chi_{CO_{R1}} + \frac{\chi_{CO_{R2}}}{2} + \frac{\chi_{CO_{R3}}}{3} + \cdots + \frac{\chi_{CO_{R20}}}{20} + \frac{\chi_{CO_{R30}}}{30}} = \frac{\chi_{CO_{R1}}}{D}$$

$$y_{C_2H_6} = \frac{n_{C_2H_6}}{n_{HCs}} = \frac{\chi_{CO_{R2}}/2}{D}$$

$$y_{C_3H_8} = \frac{n_{C_3H_8}}{n_{HCs}} = \frac{\chi_{CO_{R3}}/3}{D}$$

…

$$y_{C_{20}H_{42}} = \frac{n_{C_{20}H_{42}}}{n_{HCs}} = \frac{\chi_{CO_{R20}}/20}{D}$$

$$y_{C_{30}H_{62}} = \frac{n_{C_{30}H_{62}}}{n_{HCs}} = \frac{\chi_{CO_{R30}}/30}{D}$$

where

$$D = \frac{n_{HCs}}{n_{CO,0}}$$

The values of molar fractions of hydrocarbons are known from ASF distribution. Since $n_{CO,0}$ are the moles of CO that react in the FT reactor it can be written that the sum of the fractional conversion for all the reactions is 1.

$$\chi_{CO} = \chi_{CO_{R1}} + \chi_{CO_{R2}} + \chi_{CO_{R3}} + \cdots + \chi_{CO_{R20}} + \chi_{CO_{R30}} = 1$$

This system of equations can be solved in $\chi_{CO_{R1}}, \chi_{CO_{R2}}, \chi_{CO_{R3}}, \cdots, \chi_{CO_{R20}}, \chi_{CO_{R30}}$ and n_{HCs}.

References

[1] Michiel J.A. Tijmensen, Andre P.C. Faaij, Carlo N. Hamelinck, Martijn R.M. van Hardeveld. Exploration of the possibilities for production of Fischer Tropsch liquids and power via biomass gasification. Biomass and Bioenergy 2002;23:129–52.

[2] Hamelinck CN, Faaij APC, den Uil H, Boerrigter H. Production of FT transportation fuels from biomass; technical options, process analysis and optimisation, and development potential. Energy 2004;29:1743–71. https://doi.org/10.1016/j.energy.2004.01.002.

[3] Larson ED, Jin H, Celik FE. Large-scale gasification-based coproduction of fuels and electricity from switchgrass. Biofuels, Bioprod Biorefining 2009;3:174–94. https://doi.org/10.1002/bbb.137.

[4] Swanson RM, Platon A, Satrio JA, Brown RC. Techno-economic analysis of biomass-to-liquids production based on gasification. Fuel 2010;89. https://doi.org/10.1016/j.fuel.2010.07.027.

[5] Swanson RM. Techno-economic analysis of biomass-to-liquids production based on gasification scenarios. Iowa State University, 2009.

[6] Spyrakis S, Panopoulos KD, Kakaras E. Synthesis, modeling and exergy analysis of atmospheric air blown biomass gasification for Fischer-Tropsch process. Int J Thermodyn 2009;12:187–92.

[7] Gardezi SA, Joseph B, Prado F, Barbosa A. Thermochemical biomass to liquid (BTL) process:

Bench-scale experimental results and projected process economics of a commercial scale process. Biomass and Bioenergy 2013;59:168–86. https://doi.org/10.1016/j.biombioe.2013.09.010.

[8] Tunå P, Hulteberg C. Woody biomass-based transportation fuels - A comparative techno-economic study. Fuel 2014;117:1020–6. https://doi.org/10.1016/j.fuel.2013.10.019.

[9] Petersen AM, Farzad S, Görgens JF. Techno-economic assessment of integrating methanol or Fischer-Tropsch synthesis in a South African sugar mill. Bioresour Technol 2015;183:141–52. https://doi.org/10.1016/j.biortech.2015.02.007.

[10] Im-orb K, Simasatitkul L, Arpornwichanop A. Techno-economic analysis of the biomass gasification and Fischer-Tropsch integrated process with off-gas recirculation. Energy 2016;94:483–96. https://doi.org/10.1016/j.energy.2015.11.012.

[11] Diederichs GW, Ali Mandegari M, Farzad S, Görgens JF. Techno-economic comparison of biojet fuel production from lignocellulose, vegetable oil and sugar cane juice. Bioresour Technol 2016;216:331–9. https://doi.org/10.1016/j.biortech.2016.05.090.

[12] Snehesh AS, Mukunda HS, Mahapatra S, Dasappa S. Fischer-Tropsch route for the conversion of biomass to liquid fuels - Technical and economic analysis. Energy 2017;130:182–91. https://doi.org/10.1016/j.energy.2017.04.101.

[13] Wang WC, Liu YC, Nugroho RAA. Techno-economic analysis of renewable jet fuel production: The comparison between Fischer-Tropsch synthesis and pyrolysis. Energy 2022;239. https://doi.org/10.1016/j.energy.2021.121970.

[14] Colelli L, Segneri V, Bassano C, Vilardi G. E-fuels, technical and economic analysis of the production of synthetic kerosene precursor as sustainable aviation fuel. Energy Convers Manag 2023;288. https://doi.org/10.1016/j.enconman.2023.117165.

[15] Gao R, Zhang C, Jun KW, Kim SK, Park HG, Zhao T, et al. Transformation of CO2 into liquid fuels and synthetic natural gas using green hydrogen: A comparative analysis. Fuel 2021;291. https://doi.org/10.1016/j.fuel.2020.120111.

[16] Adelung S, Maier S, Dietrich RU. Impact of the reverse water-gas shift operating conditions on the Power-to-Liquid process efficiency. Sustain Energy Technol Assessments 2021;43. https://doi.org/10.1016/j.seta.2020.100897.

[17] Zang G, Sun P, Elgowainy AA, Bafana A, Wang M. Performance and cost analysis of liquid fuel production from H2and CO2based on the Fischer-Tropsch process. J CO2 Util 2021;46. https://doi.org/10.1016/j.jcou.2021.101459.

[18] Sandeep K, Dasappa S. Oxy-steam gasification of biomass for hydrogen rich syngas production using downdraft reactor configuration. Int J Energy Res 2014;38:174–88. https://doi.org/10.1002/er.3019.

[19] Smith JM. Introduction to chemical engineering thermodynamics. Eight. 2018.